Visual PET/CT scoring of mesenteric FDG uptake to differentiate between tuberculous peritonitis and peritoneal carcinomatosis

Shao-bo Wang ⓘ
Hong He ⓘ
Dong-dong Xv ⓘ
Bo She ⓘ
Ren-cai Lu ⓘ
Zhao-hui Yang ⓘ
Hong Shi ⓘ
Ran Xie ⓘ

PURPOSE

We aimed to differentiate tuberculous peritonitis (TBP) from peritoneal carcinomatosis (PC) using a visual positron-emission tomography/computed tomography (PET/CT) scoring system based on mesenteric fluorodeoxyglucose (FDG) uptake.

METHODS

PET/CT scans from 31 patients with TBP and 92 patients with PC were retrospectively reviewed. A visual PET/CT scoring system for mesenteric FDG uptake was used according to the following characteristics: FDG uptake intensity (low = 0, moderate = 1, high = 2), FDG uptake deposits (uniform = 0, irregular = 1, ascitic = 2), FDG uptake focality (diffuse = 0, segmental = 1, focal = 2), nodularity on the corresponding CT (nonnodular = 0, micronodular = 1, macronodular = 2) and mesenteric lymphadenopathy (absent = 0, lymphadenopathy without FDG uptake = 1, lymphadenopathy with FDG uptake = 2). The FDG uptake intensity, deposits, focality, nodularity and mesenteric lymphadenopathy scores between TBP and PC were compared using chi-square tests. The diagnostic performance of this scoring system for differentiating TBP from PC was analyzed using a receiver operating characteristic (ROC) curve. $P < 0.05$ was considered statistically significant.

RESULTS

Twenty-four patients with TBP (77.4%) and 56 patients with PC (60.9%) had mesenteric FDG uptake ($P = 0.095$) and were included for evaluation with the visual PET/CT scoring system. PC lesions scored higher than TBP lesions in FDG uptake deposits ($P < 0.001$), focality ($P < 0.001$) and nodularity ($P < 0.001$). No significant differences were observed between PC and TBP lesions in FDG uptake intensity ($P = 0.396$) and lymphadenopathy ($P = 0.074$). The total score that combined deposits, focality and nodularity had significant value for differentiating TBP from PC (area under the curve (AUC) = 0.869, $P < 0.001$), and a cutoff > 1 had a sensitivity (the accuracy for diagnosis of PC) of 80.4% and a specificity (the accuracy for diagnosis of TBP) of 75.0%.

CONCLUSION

A visual PET/CT scoring system based on mesenteric FDG uptake performed well in differentiating between TBP and PC.

From Yunnan Key Laboratory of Primate Biomedical Research, Institute of Primate Translational Medicine (S.B.W., Z.H.Y.,H.S.), Kunming University of Science and Technology, Kunming, China; PET/CT center (S.B.W., H.H., D.D.X., B.S., R.C.L.), First People's Hospital of Yunnan Province, Kunming, China; PET-CT Center (R.X. ✉ *340676718@qq.com*), Yunnan Cancer Hospital, Kunming, China.

D ifferentiating between tuberculous peritonitis (TBP) and peritoneal carcinomatosis (PC) is difficult because of the overlap in the clinical, laboratory and radiological findings between the two entities (1, 2). Delayed effective treatment may cause morbidity and mortality in some cases. Laparoscopy, laparotomy, and peritoneal biopsy have been advocated as the confirmed methods for a differential diagnosis, but these procedures are invasive and may cause some complications. Thus, identifying feasible predictors to differentiate TBP from PC without surgical intervention is necessary (3).

Positron-emission tomography/computed tomography (PET/CT) is more useful than magnetic resonance imaging (MRI) and CT (4–6) for detecting peritoneal diseases. PET/CT has been used as a noninvasive tool to further evaluate ascites (7, 8) and peritoneal thickening (9) after conventional laboratory and radiological examinations.

TBP commonly shows epithelioid granulomata with caseation and/or mycobacterial infection (10). Similar to neoplasms, nonneoplastic conditions, such as infection, inflammation, and granulomatous diseases, also appear to have elevated glycolysis and are therefore

readily visualized by fluorodeoxyglucose (FDG) PET/CT imaging (11). However, the clinical dilemma is that TBP lesions might present with similar FDG uptake to that of PC lesions on PET/CT imaging (12), which poses the clinical question of whether PET/CT should be performed after CT and/or MRI and how PET/CT can be used to differentiate between TBP and PC. Interestingly, our previous study demonstrated that certain PET/CT findings in the parietal peritoneum, a key component of the peritoneum, were useful in differentiating TBP from PC (13).

The mesentery, another key component of the peritoneum, is a fan-shaped, double peritoneal fold that suspends the ileal and jejunal small bowel loops from the posterior abdominal wall. The mesentery contains vascular and lymphatic structures and encases the suspended bowel loops, forming a visceral peritoneal coat. The mesentery is also a common site of extension of neoplastic and inflammatory disease from adjacent organs or systemic disease because this structure is easily accessed by ascites and has an abundance of mesenteric ruffles, peripheral vessels and lymphoid aggregates (14–16). Thus, whether mesenteric PET/CT should be used and how the PET/CT findings can differentiate between TBP and PC is worthy of investigation.

Methods

Study cohort

This study was approved by the Institutional Review Board of the Yunnan Cancer Hospital (No. QT201921). The requirement for informed consent was waved due to the retrospective nature of this study. The medical records of patients with TBP and PC who underwent pre-therapy PET/CT from June 2014 to February 2019 at the Yunnan Cancer Hospital were reviewed. We enrolled 31 consecutive patients (male/female, 10/21; age, 49.8±15.0 years) who showed

---

Main points

- Mesenteric PET/CT scoring system helps differentiate tuberculous peritonitis (TBP) from peritoneal carcinomatosis (PC).

- Uniform deposits, diffuse FDG uptake and nonnodular findings in the mesentery are significant features of TBP.

- Ascitic deposits, segmental and focal FDG uptake and macronodular findings in the mesentery are significant features of PC.
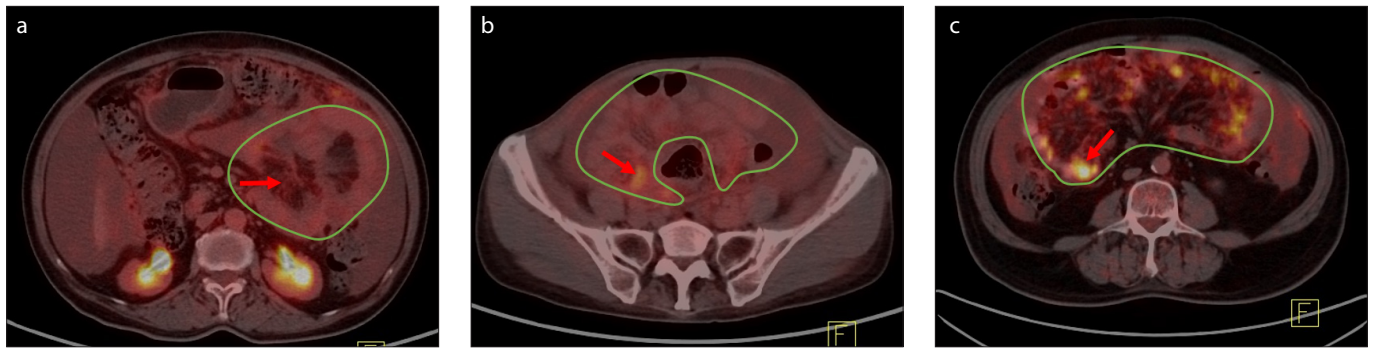
---

peritoneal FDG uptake and whose diagnoses were pathologically confirmed as TBP by surgery (n=14) or laparoscopy (n=17). For these patients, TB lesions were detected beyond the peritoneum, including the ovary (n=18), cervical (n=2), thoracic (n=9) and abdominal (n=12) lymph nodes, lung (n=8), and endometrium (n=1).

We also enrolled 92 consecutive patients (male/female, 13/79; age, 61.0±11.3 years) who showed peritoneal FDG uptake and whose diagnoses were pathologically confirmed as PC by surgery (n=51), laparoscopy (n=37), or ascites cytology (n=4). For these patients with PC, the tumor origins were the ovary (n=48), stomach (n=6), colon (n=4), pancreas (n=3), lung (n=2), and appendix (n=1); 19 tumors were of an undetermined origin.

Image acquisition

PET/CT scanning was performed with a Siemens Biograph 16 PET/CT scanner (Siemens Medical Solutions). ^{18}F was produced in an HM-10 cyclotron (Sumitomo Heavy Industries). ^{18}F-FDG was automatically synthesized in a chemical synthesis module (Beijing PET Biotechnology Co., Ltd.) with a radiochemical purity >95%. After fasting for more than 6 h in a calm state, patients were intravenously injected with 0.15 mCi (5.5 MBq)/kg ^{18}F-FDG and then laid down in a dark room for approximately 1 h.

PET and unenhanced CT imaging were performed after the patients emptied their urinary bladders. Scanning was performed from the middle of the femur to the cranial vault. The PET images were reconstructed according to an iterative ordered subset expectation maximization method. The reconstruction thickness of the CT images was 3.0 mm, and the PET and CT images were transferred to a Syngo MMWP workstation (Siemens Medical Solutions) to display frame-on-frame fusion images.

Imaging analysis

All PET/CT findings were separately reviewed by two readers who were blinded to the clinical data and other imaging examinations. If interpretive disagreements occurred, the final report was decided by a third reader. Each reader had more than 5 years of experience with PET/CT.

The confirmation of mesenteric FDG uptake on PET/CT was based on the requisite exclusion of physiologic bowel activity, retained urinary activity, misregistration artifacts, attenuation correction artifacts,

intestine peristalsis artifacts, and FDG uptake from the viscera, visceral peritoneum, omentum, parietal peritoneum, and other peritoneal structures. The presence of concomitant lymphadenopathy in the mesentery was additionally noted.

The standardized uptake value (SUV) was measured by drawing a region of interest (ROI) along the margin of the mesenteric lesion with the most intensive FDG uptake. Because the maximum SUV (SUVmax) was significantly more reproducible than the mean SUV, the SUVmax was used for the semiquantitative analysis of mesenteric FDG uptake in this study.

In addition, a visual analysis was used to score the FDG uptake intensity. Low intensity is less than the liver uptake (score = 0), moderate intensity is closer to the liver uptake (score = 1), and high intensity is more than the liver uptake (score = 2) (Fig. 1).

The FDG uptake deposits (ascitic, irregular and uniform) were classified based on the anatomical characteristics of the mesentery. The small bowel mesentery emerges from the "root region" (as named by Treves), which corresponds to the attachment of the superior mesenteric artery to the aorta. The distal mesentery extends radially up to the intestinal margin (17). The mesentery suspends the jejunum and ileum and is divided into five parts: the upper part of the jejunum, the lower part of the jejunum, the upper part of the ileum, the middle part of the ileum, and the lower part of the ileum.

Because of the natural flow of fluid in the peritoneal cavity, the lower part of the ileal mesentery in the pelvic cavity was a common site of ascitic deposits (18, 19). Thus, the mesenteric FDG uptake deposits were classified into ascitic deposits where FDG uptake was completely or dominantly located in the lower part of the ileal mesentery (score = 0), uniform deposits where FDG uptake was uniformly located in almost the entire mesentery of the small bowel (score = 1), and irregular deposits with neither ascitic nor uniform deposits (score = 2) (Fig. 2).

The FDG uptake focality (focal, segmental and diffuse) was also used to describe mesenteric FDG uptake. Focal uptake was defined as isolated or sporadic FDG uptake in the small bowel mesentery (score = 2), segmental uptake was defined as nonfocal FDG uptake extending to no more than one of the five parts of the small bowel mesentery (score = 1), and diffuse uptake was defined as nonfocal FDG uptake that extends to more than one of the five parts of the small

Figure 1. a–c. The patterns of FDG uptake intensity in the mesentery. To avoid misinterpreting the FDG uptake in abdominal organs and other peritoneal structures, the small bowel and mesentery were delineated in green according to the continuous sectional images. Cross-sectional PET/CT fusion image **(a)** from a 74-year-old female patient with PC from ovarian cancer shows low uptake in the mesentery (score = 0, *red arrow*); cross-sectional PET/CT fusion image **(b)** from a 52-year-old female patient with PC from ovarian cancer shows moderate uptake in the mesentery (score = 1, *red arrow*); cross-sectional PET/CT fusion image **(c)** from an 80-year-old female patient with PC from ovarian cancer shows high uptake in the mesentery (score = 2, *red arrow*).
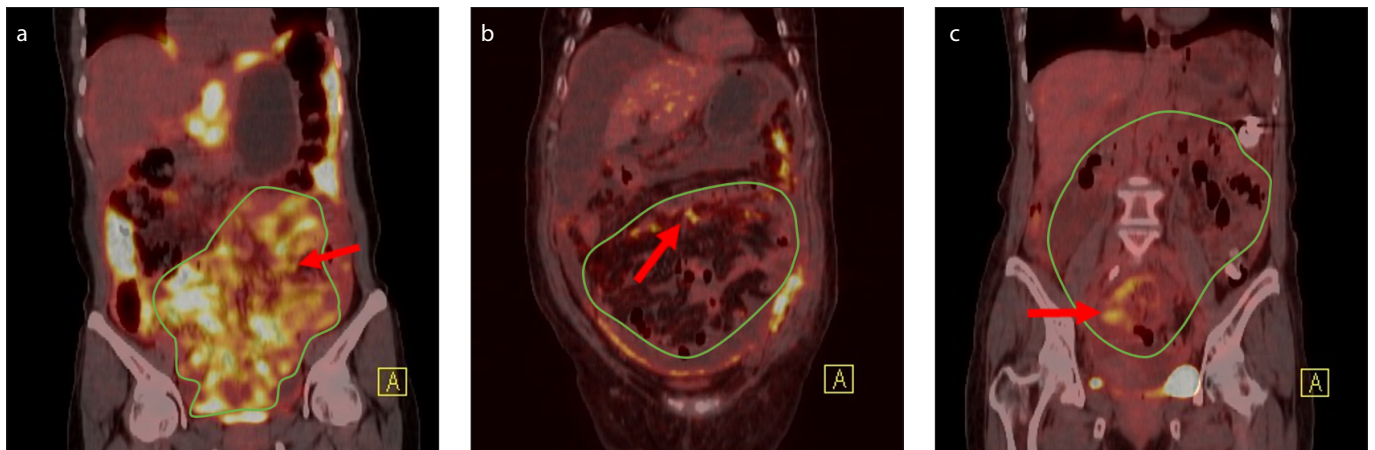

Figure 2. a–c. The patterns of FDG uptake deposits in the mesentery. To avoid misinterpreting the FDG uptake by abdominal organs and other peritoneal structures, the small bowel and mesentery were delineated in green according to the continuous sectional images. Coronal sectional PET/CT fusion image **(a)** from a 50-year-old female patient with TBP shows uniform deposits in the mesentery (score = 0, *red arrow*); coronal sectional PET/CT fusion image **(b)** from an 84-year-old female patient with PC from ovarian cancer shows irregular deposits in the mesentery (score = 1, *red arrow*); coronal sectional PET/CT fusion image **(c)** from a 57-year-old female patient with PC from ovarian cancer shows ascitic deposits in the mesentery (score = 2, *red arrow*).

bowel mesentery (score = 0) (Fig. 3). If multiple patterns coexisted in one patient, a diffuse pattern accompanied by a segmental and/or focal pattern was noted as a diffuse pattern, and a segmental pattern accompanied by a focal pattern was noted as a segmental pattern.

Nodularity (nonnodular findings, micronodules and macronodules) was used to describe the corresponding CT findings of the mesenteric FDG uptake. Nonnodular was defined as the absence of nodules (score = 0), micronodular was defined as a single lesion <5 mm in diameter (score = 1), and macronodular was defined as a single lesion ≥5 mm in diameter (score = 2). If multiple patterns coexisted in one patient, macronodules accompanied by micronodules and/or nonnodular findings were noted as macronodules, and micronodules accompanied by nonnodular findings were noted as micronodules (Fig. 4).

Lymphadenopathy was defined as enlargement of the lymph nodes (1 cm or more) or an alteration in the consistency and/or number of lymph nodes (18). The concomitant lymphadenopathy in the mesentery was classified as the absence of lymphadenopathy (score = 0), lymphadenopathy without FDG uptake (score = 1) or lymphadenopathy with FDG uptake (score = 2) (Fig. 5).

The patients with mesenteric FDG uptake were included for evaluation with the visual PET/CT scoring system, and the remaining patients were not included. The PET/CT pattern score was defined according to the visual analysis of the predisposition to imaging characteristics, and the details are shown in Table 1.

Statistical analysis

Statistical analyses were performed using MedCalc, version 13.0.0.0 (MedCalc Soft-

ware). The interrater agreement test was used to evaluate the visual scores from the two readers, and the diagnostic concordance was statistically significant if the *kappa* value was > 0.75. The SUVmax measurements between TBP and PC were compared using *t* tests, and the FDG uptake intensity, deposits, focality, nodularity and mesenteric lymphadenopathy scores between TBP and PC were compared using chi-square tests. The diagnostic performance of this scoring system for differentiating TBP from PC was analyzed using a receiver operating characteristic (ROC) curve. If $P < 0.05$, the difference was considered statistically significant.

Results

Mesenteric FDG uptake was observed in 77.4% (24/31) of the patients with TBP and in 60.9% (56/92) of the patients with PC ($P = 0.095$). The concordance between the two readers in determining the visual
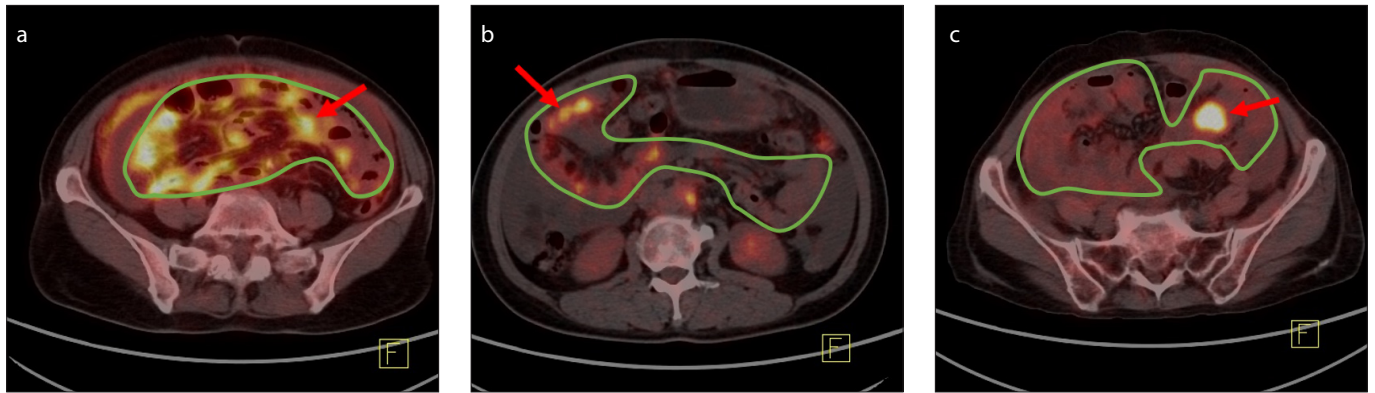
Figure 3. a–c. The patterns of FDG uptake focality in the mesentery. To avoid misinterpreting the FDG uptake by abdominal organs and other peritoneal structures, the small bowel and mesentery were delineated in green according to the continuous sectional images. Cross-sectional PET/CT fusion image **(a)** from a 66-year-old female patient with TBP shows diffuse uptake in the mesentery (score = 0, *red arrow*); cross-sectional PET/CT fusion image **(b)** from a 49-year-old female PC from ovarian cancer shows segmental uptake (score = 1, *red arrow*) in the mesentery; cross-sectional PET/CT fusion image **(c)** from an 80-year-old female patient with PC from ovarian cancer shows focal uptake (score = 2, *red arrow*) in the mesentery.
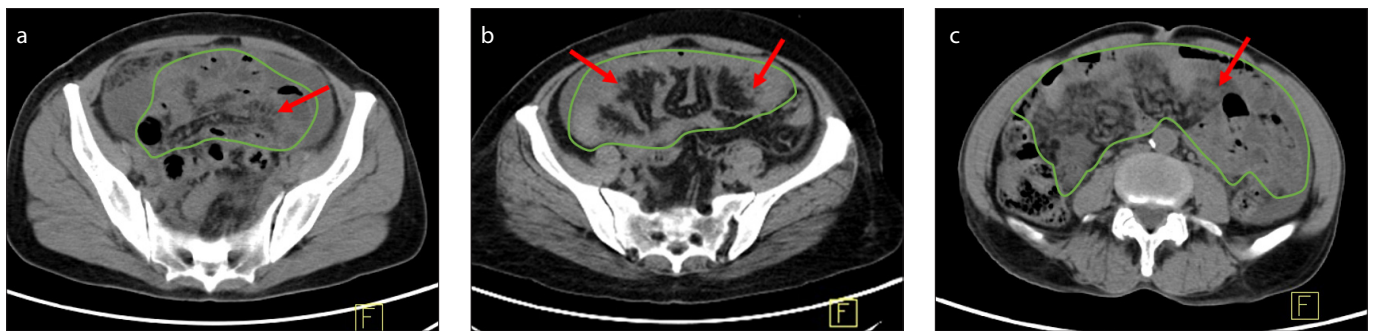

Figure 4. a–c. The patterns of FDG uptake nodularity in the mesentery. To avoid misinterpreting the FDG uptake by abdominal organs and other peritoneal structures, the small bowel and mesentery were delineated in green according to the continuous sectional images. Cross-sectional CT image **(a)** from a 47-year-old female patient with TBP shows nonnodular findings in the mesentery (score = 0, *red arrow*); cross-sectional CT image **(b)** from a 50-year-old female patient with TBP shows micronodular findings in the mesentery (score = 1, *red arrow*); cross-sectional CT image **(c)** from a 64-year-old male patient with PC from pancreatic cancer shows macronodular findings in the mesentery (score = 2, *red arrow*).
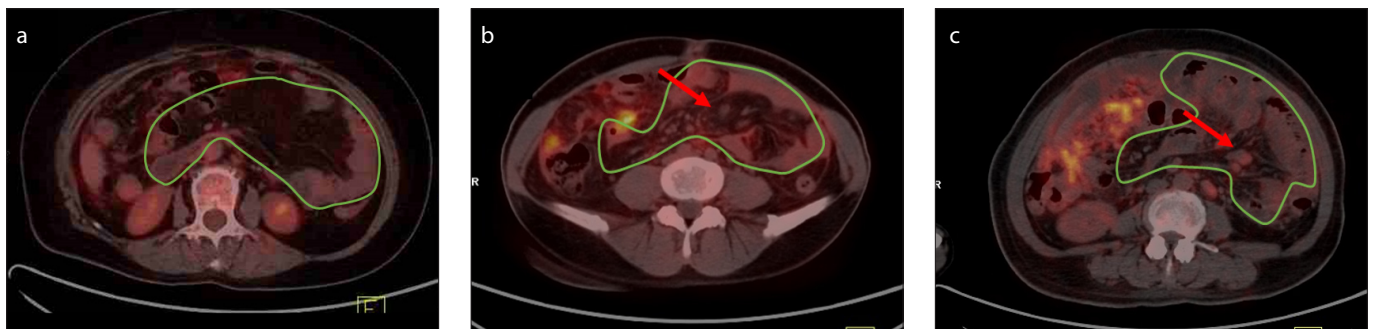

Figure 5. a–c. The patterns of mesenteric lymphadenopathy. To avoid misinterpreting the FDG uptake by abdominal organs and other peritoneal structures, the small bowel and mesentery were delineated in green according to the continuous sectional images. Cross-sectional PET/CT fusion image **(a)** from a 60-year-old female patient with PC of an undetermined origin shows the absence of mesenteric lymphadenopathy (score = 0); cross-sectional PET/CT fusion image **(b)** from a 44-year-old female patient with TBP shows mesenteric lymphadenopathy without FDG uptake (score = 1, *red arrow*); cross-sectional PET/CT fusion image **(c)** from a 62-year-old female patient with PC from ovarian cancer shows mesenteric lymphadenopathy with FDG uptake (score = 2, *red arrow*).

PET/CT scores was strong, with *kappa* values of 0.782, 0.920, 0.834, 0.782 and 0.754 for FDG uptake intensity, deposits, focality, nodularity on corresponding CT, and mesenteric lymphadenopathy, respectively. The PET/CT findings of TBP and PC are shown in Table 2.

The mean SUVmax measurements were 4.8±1.9 and 4.6±2.5 in 24 patients with TBP and 56 patients with PC, respectively ($P = 0.284$). No differences were observed between TBP and PC in FDG uptake intensity from the visual analysis ($P = 0.396$).

A significant difference was observed in FDG uptake deposits between TBP and PC ($P < 0.001$). Uniform deposits were more commonly observed in patients with TBP than in patients with PC (83.3% vs. 23.2%,

$P < 0.001$), irregular deposits were less commonly observed in patients with TBP than in patients with PC (8.3% vs. 30.4%, $P = 0.034$), and ascitic deposits were less commonly observed in patients with TBP than in patients with PC (8.3% vs. 46.4%, $P = 0.001$).

A significant difference was observed in FDG uptake focality between TBP and PC ($P < 0.001$). Diffuse FDG uptake on PET/CT oc-

Table 1. Components and definitions of the PET/CT score for mesenteric FDG uptake to differentiate between TBP and PC

PET/CT characteristics	Qualitative definition of the characteristics	Score
Intensity		
Low	Less than the liver uptake	0
Moderate	Closer to the liver uptake	1
High	Higher than the liver uptake	2
Deposits		
Uniform	FDG uptake uniformly located in almost the entire small bowel	0
Irregular	Neither uniform nor ascitic uptake	1
Ascitic	FDG uptake completely or dominantly located in the lower part of the ileum	2
Focality		
Diffuse	≥ One of the five parts of the mesentery in length	0
Segmental	< One of the five parts of the mesentery in length	1
Focal	Isolated or discrete FDG uptake	2
Nodularity		
Nonnodular	Absence of nodules	0
Micronodular	< 5 mm in diameter	1
Macronodular	≥ 5 mm in diameter	2
Lymphadenopathy		
Absent	Absence of mesenteric lymphadenopathy	0
Lymphadenopathy without FDG uptake	Mesenteric lymphadenopathy without elevated FDG uptake	1
Lymphadenopathy with FDG uptake	Mesenteric lymphadenopathy with elevated FDG uptake	2

PET/CT, positron emission tomography/computed tomography; FDG, fluorodeoxyglucose; TBP, tuberculous peritonitis; PC, peritoneal carcinomatosis.

curred in 79.2% of the patients with TBP and in 28.6% of the patients with PC ($P < 0.001$). Segmental FDG uptake occurred in 12.5% of the patients with TBP and 33.9% of the patients with PC ($P = 0.049$). Focal FDG uptake occurred in 8.3% of the patients with TBP and in 37.5% of the patients with PC ($P = 0.008$).

A significant difference was observed in nodularity on the corresponding CTs between TBP and PC ($P < 0.001$). Nonnodular findings were observed in 66.7% of patients with TBP and 26.8% of patients with PC ($P = 0.001$), micronodules were observed in 29.2% of patients with TBP and 28.6% of patients with PC ($P = 0.957$), and macronodules were observed in 4.2% of patients with TBP and 44.6% of patients with PC ($P < 0.001$).

No significant difference was observed in mesenteric lymphadenopathy between TBP and PC ($P = 0.074$).

As shown in Table 3, the areas under the ROC curve (AUCs), from high to low, were 0.869 for a combined deposits-focality-nodularity score, 0.807 for deposits score, 0.762 for focality score, 0.759 for nodularity score, 0.613 for lymphadenopathy score, and 0.589 for intensity score.

A combined deposits-focality-nodularity score yielded the highest diagnostic performance for differentiating TBP from PC. According to pairwise comparison of ROC curves, the combined deposits-focality-nodularity score had a higher diagnostic performance than the intensity score ($P = 0.002$), focality score ($P < 0.000$), nodularity score ($P = 0.016$) and lymphadenopathy score ($P = 0.001$); no significant differences were observed between the diagnostic performances the combined deposits-focality-nodularity score and deposits score ($P = 0.091$). By using a cutoff >1 for a combined deposits-focality-nodularity score to differentiate between TBP and PC, the sensitivity (the accuracy for diagnosing PC) was 80.4%, and the specificity (the accuracy for diagnosing TBP) was 75%.

Discussion

This was a preliminary study designed to describe FDG uptake patterns in the small bowel mesentery between TBP and PC. A scoring system for FDG uptake intensity, deposits, focality, nodularity and concomitant lymphadenopathy was introduced to rate mesenteric involvement, and the results had a strong concordance between the two

readers (all *kappa* values >0.750), which ensured diagnostic reproducibility.

This study showed that mesenteric FDG uptake on PET/CT was noted in 77.4% of the patients with TBP and in 60.9% of the patients with PC, and no significant differences were observed between the two entities ($P = 0.095$). Another published study reported that mesenteric changes on CT were detected in 88.9%–100% of the patients with TBP and 37.3%–70% of the patients with PC (20–22). This difference might result from the different imaging principles between PET and CT. PET evaluates the metabolic and molecular characteristics of lesions but is limited in visualizing anatomical structures, while CT evaluates anatomical structures but cannot visualize the metabolic and molecular aspects of lesions (23).

The role of PET/CT for differentiating TBP from PC is rarely reported. The positive rate for the diagnosis of PC was 86.3% if only using FDG uptake in the parietal peritoneum, while the false-positive rate for the diagnosis of TBP reached 100% (13). Special attention should be paid to peritoneal tuberculosis, which has a high FDG uptake and may mimic malignant peritoneal thickening (9).

Although CT remains the dominant imaging modality for patients with intra-abdominal disease, CT does not accurately detect mesenteric lesions (15, 24, 25). PET/CT has the potential to improve the detection of peritoneal lesions with FDG uptake due to low background activity, and fused PET/CT images offer the combined benefits of anatomic and functional imaging. The correlation of uptake between modalities indicating the pathogenesis of intraperitoneal spread provides a rational system of analysis and is essential to defining disease (26).

In this study, both the semiquantitative index and rating score of FDG uptake for mesenteric seeding were not significantly different between TBP and PC. Most PC showed high FDG uptake, which used to be interpreted with the Warburg effect that cancer cells use glucose by aerobic glycolysis in the presence of ample oxygen. However, Li et al. (27, 28) demonstrated that ascites carcinomas are severely hypoxic in the mouse model, and FDG uptake increases in hypoxic but not normoxic cancer, which might be explained by the anaerobic glycolysis pathway rather than "aerobic glycolysis" of glucose metabolism. TBP showed high FDG uptake because TB lesions contain many epithelioid cells, lymphocytes, and Langerhans cells that have a high expression levels of glucose transporter (Glut)-1 and Glut-3 (13).

Therefore, many reports have shown that peritoneal TB cannot be differentiated from PC using FDG PET/CT (29, 30). However, by visualizing the lesions with PET, this study demonstrated that FDG uptake deposits and focality were significantly different between TBP and PC (both $P < 0.001$), which might be related to different mechanisms of mesenteric lesion spread.

TBP is usually secondary to the hematogenous spread of tubercles (10, 31) and may present as disseminated TB (32). Hematogenous spread cannot be restricted and can be widespread. As shown in this study, uniform deposits and diffuse uptake might be considered significant features of TBP (both $P < 0.001$).

The dissemination feature of peritoneal carcinomatosis might be related to a different primary tumor. According to the hypothesis by Deraco et al. (33), random and proximal dissemination is seen in most tumors, such as colorectal cancer, gastric cancer and serous ovarian cancer, while widespread dissemination is seen in relatively rare tumors, such as mucinous colorectal cancer, diffuse gastric cancer and mucinous ovarian cancer. This might be one of the reasons accounting for the local spread of PC.

PC occurs frequently by peritoneal seeding and features locoregional cancer spread because the peritoneum acts as a first-line defense against host resistance to PC (14). Peritoneal seeding is a multistep process: The neoplastic cells must first gain access to the peritoneal cavity, spread transcoelomically along with peritoneal fluid, attach to the mesothelial surface, and then invade through the peritoneal surface. Peritoneal seeding can spread across distances but is restricted by gravity, intestinal peristalsis, and the anatomic features of the abdominal compartment. For the mesentery, the lower part of the ileum is a common site of ascitic deposits in the peritoneal cavity (12,

Table 2. PET/CT scores of mesenteric FDG uptake in 24 patients with TBP and 56 patients with PC

PET/CT characteristics	Score	TBP, n (%)	PC, n (%)	P *
Intensity		24	56	0.396
Low	0	4 (16.7)	16 (28.6)	
Moderate	1	7 (29.2)	18 (32.1)	
High	2	13 (54.2)	22 (39.3)	
Deposits				<0.001
Uniform	0	20 (83.3)	13 (23.2)	
Irregular	1	2 (8.3)	17 (30.4)	
Ascitic	2	2 (8.3)	26 (46.4)	
Focality				<0.001
Diffuse	0	19 (79.2)	16 (28.6)	
Segmental	1	3 (12.5)	19 (33.9)	
Focal	2	2 (8.3)	21 (37.5)	
Nodularity				<0.001
Nonnodular	0	16 (66.7)	15 (26.8)	
Micronodular	1	7 (29.2)	16 (28.6)	
Macronodular	2	1 (4.2)	25 (44.6)	
Lymphadenopathy				0.074
Absent	0	7 (29.2)	31 (55.4)	
Without FDG uptake	1	8 (33.3)	9 (16.1)	
With FDG uptake	2	9 (37.5)	16 (28.6)	

*Pearson chi-square test.
PET/CT, positron emission tomography/computed tomography; FDG, fluorodeoxyglucose; TBP, tuberculous peritonitis; PC, peritoneal carcinomatosis.

Table 3. The diagnostic performance of the mesenteric PET/CT scoring system in differentiating TBP from PC

Parameter	Intensity	Deposits	Focality	Nodularity	Lymphadenopathy	Deposits-Focality-Nodularity
Area under the curve	0.589	0.807	0.762	0.759	0.613	0.869
Cutoff (score)	≤ 1	> 0	> 0	> 1	≤ 0	> 1
Sensitivity (%)	60.7	76.8	71.4	44.6	55.4	80.4
Specificity (%)	54.2	83.3	79.1	95.8	70.8	75.0

PET/CT, positron emission tomography/computed tomography; TBP, tuberculous peritonitis; PC, peritoneal carcinomatosis.

13), and lymphoid aggregates are extremely plentiful in the area of the terminal ileum that facilitates ascites resorption, brings cancer cells to the open stomas and facilitates adherence, implantation, and then progression (14).

As suggested by this study, ascitic deposits and focal and segmental FDG uptake might be useful predictors of PC ($P = 0.001$, $P = 0.008$, and $P = 0.049$, respectively).

The size of mesenteric nodules on CT images is a common feature for differentiating TBP and PC, but previous studies found inconsistent results. Hyun et al. (21) reported that macronodules (≥5 mm in diameter) were much more frequently observed in patients with TBP (52%) than in patients with PC (12%). However, Charoensak et al. (20) reported macronodules (≥10 mm in diameter) in 6.7% of patients with TBP and 28.6% of patients with PC; 93.3% of patients with TBP and 71.4% of patients with PC showed micronodules. Seung et al. (34) reported mesenteric micronodules in 44.4% of the patients with TBP; none of the patients with TBP showed macronodules, and 48.0% of patients with PC showed mesenteric nodules that were composed of micronodules and macronodules.

For the visual diagnosis with laparoscopy, TBP presents multiple yellowish white micronodules of uniform size (usually <5 mm), and PC presents macronodules (1 to 5 cm in diameter) on the peritoneal surface (35). These findings with laparoscopy seem to support the findings of Charoensak et al. (20) and Seung et al. (34).

After carefully reviewing these reports, apart from different CT diagnostic standards regarding the size of nodules, we found that this inconsistency might have resulted from Hyun et al. (21) incorporating mesenteric lymphadenopathy into mesenteric nodules, but not Charoensak et al. (20) and Seung et al. (34).

This study demonstrated that FDG uptake nodularity is significantly different between TBP and PC ($P < 0.001$). Macronodules showed more commonly in PC than in TBP (44.6% and 4.2%, $P < 0.001$, respectively) and can be regarded as a significant feature of PC. Micronodules did not reach a significant difference (28.6% and 29.2%, $P = 0.957$, respectively). Nonnodular findings showed in 66.7% of the patients with TBP and in 26.8% of the patients with PC ($P = 0.001$) and can be considered an important predictor of TBP.

With the help of CT, routine evaluations of the mesenteric lymph nodes are possible. Normal mesenteric lymph nodes are routinely identified alongside the mesenteric vessels at the mesenteric root and throughout the mesentery (36). Thus, mesenteric lymphadenopathy was considered a concomitant finding that was excluded from mesenteric nodules in this study. Unfortunately, the presence of mesenteric lymphadenopathy was not significantly different between TBP and PC in this study ($P = 0.074$).

As shown in this study, the deposits, focality and nodularity scores of mesenteric FDG uptake are significant indicators for differentiating TBP from PC, and a combination of these indicators has the highest diagnostic performance, with a sensitivity of 80.4% and a specificity of 75%.

Our study has limitations. The number of female patients is relatively high due to the specialization in gynecological oncology in this hospital. Furthermore, the study is retrospective and from a single institution. Additionally, this study reveals PET/CT findings only in the mesentery; further studies need to investigate PET/CT findings in other peritoneal components to enhance this differential diagnosis.

In conclusion, this study presented a useful PET/CT scoring system for mesenteric involvement with FDG uptake to differentiate between TBP and PC. This scoring system could help further answer the clinically challenging question of whether PET/CT should be performed and how PET/CT can differentiate between TBP and PC.

References
1. Cavalli Z, Ader F, Valour F, et al. Clinical presentation, diagnosis, and bacterial epidemiology of peritoneal tuberculosis in two university hospitals in France. Infect Dis Ther 2016; 5:193–199. [Crossref]
2. Guirat A, Koubaa M, Mzali R, et al. Peritoneal tuberculosis. Clin Res Hepatol Gastroenterol 2011; 35:60–69. [Crossref]
3. Kaya M, Kaplan MA, Isikdogan A, Celik Y. Differentiation of tuberculous peritonitis from peritonitis carcinomatosa without surgical intervention. Saudi J Gastroenterol 2011; 17:312–327. [Crossref]
4. Satoh Y, Ichikawa T, Motosugi U, et al. Diagnosis of peritoneal dissemination: comparison of 18F-FDG PET/CT, diffusion-weighted MRI, and contrast-enhanced MDCT. AJR Am J Roentgenol 2011; 196:447–453. [Crossref]
5. Sanli Y, Turkmen C, Bakir B, et al. Diagnostic value of PET/CT is similar to that of conventional MRI and even better for detecting small peritoneal implants in patients with recurrent ovarian cancer. Nucl Med Commun 2012; 33:509–515. [Crossref]
6. Kyriazi S, Kaye SB, deSouza NM. Imaging ovarian cancer and peritoneal metastases--current and emerging techniques. Nat Rev Clin Oncol 2010; 7:381–393. [Crossref]
7. Zhang M, Jiang X, Zhang M, Xu H, Zhai G, Li B. The role of 18F-FDG PET/CT in the evaluation of ascites of undetermined origin. J Nucl Med 2009; 50:506–512. [Crossref]
8. Han N, Sun X, Qin C, et al. Value of (18)F-FDG PET/CT combined with tumor markers in the evaluation of ascites. AJR Am J Roentgenol 2018; 210:1155–1163. [Crossref]
9. Chen R, Chen Y, Liu L, Zhou X, Liu J, Huang G. The Role of (1)(8)F-FDG PET/CT in the evaluation of peritoneal thickening of undetermined origin. Medicine (Baltimore) 2016; 95:e3023. [Crossref]
10. Sanai FM, Bzeizi KI. Systematic review: tuberculous peritonitis--presenting features, diagnostic strategies and treatment. Aliment Pharmacol Ther 2005; 22:685–700. [Crossref]
11. Hashefi M, Curiel R. Future and upcoming non-neoplastic applications of PET/CT imaging. Ann N Y Acad Sci 2011; 1228:167–174. [Crossref]
12. Shimamoto H, Hamada K, Higuchi I, et al. Abdominal tuberculosis: peritoneal involvement shown by F-18 FDG PET. Clin Nucl Med 2007; 32:716–718. [Crossref]
13. Wang SB, Ji YH, Wu HB, et al. PET/CT for differentiating between tuberculous peritonitis and peritoneal carcinomatosis: The parietal peritoneum. Medicine (Baltimore) 2017; 96:e5867. [Crossref]
14. Sugarbaker PH. Peritoneum as the first-line of defense in carcinomatosis. J Surg Oncol 2007; 95:93–96. [Crossref]
15. Valle M, Garofalo A. Laparoscopic staging of peritoneal surface malignancies. Eur J Surg Oncol 2006; 32:625–627. [Crossref]
16. Hamrick-Turner JE, Chiechi MV, Abbitt PL, Ros PR. Neoplastic and inflammatory processes of the peritoneum, omentum, and mesentery: diagnosis with CT. Radiographics 1992; 12:1051–1068. [Crossref]
17. Coffey JC, O'Leary DP. The mesentery: structure, function, and role in disease. Lancet Gastroenterol Hepatol 2016; 1:238–247. [Crossref]
18. Sheth S, Horton KM, Garland MR, Fishman EK. Mesenteric neoplasms: CT appearances of primary and secondary tumors and differential diagnosis. Radiographics 2003; 23:457–473. [Crossref]

19. Silverman PM. The subperitoneal space: mechanisms of tumour spread in the peritoneal cavity, mesentery, and omentum. Cancer Imaging 2003; 4:25–29. [Crossref]

20. Charoensak A, Nantavithya P, Apisarnthanarak P. Abdominal CT findings to distinguish between tuberculous peritonitis and peritoneal carcinomatosis. J Med Assoc Thai 2012; 95:1449–1456.

21. Ha HK, Jung JI, Lee MS, et al. CT differentiation of tuberculous peritonitis and peritoneal carcinomatosis. AJR Am J Roentgenol 1996; 167:743–748. [Crossref]

22. Na-ChiangMai W, Pojchamarnwiputh S, Lertprasertsuke N, Chitapanarux T. CT findings of tuberculous peritonitis. Singapore Med J 2008; 49:488–491.

23. Seemann MD. PET/CT: fundamental principles. Eur J Med Res 2004; 9:241–246.

24. Yan TD, Morris DL, Shigeki K, Dario B, Marcello D. Preoperative investigations in the management of peritoneal surface malignancy with cytoreductive surgery and perioperative intraperitoneal chemotherapy: Expert consensus statement. J Surg Oncol 2008; 98:224–227. [Crossref]

25. Low RN, Semelka RC, Worawattanakul S, Alzate GD, Sigeti JS. Extrahepatic abdominal imaging in patients with malignancy: comparison of MR imaging and helical CT, with subsequent surgical correlation. Radiology 1999; 210:625–632. [Crossref]

26. De Gaetano AM, Calcagni ML, Rufini V, Valenza V, Giordano A, Bonomo L. Imaging of peritoneal carcinomatosis with FDG PET-CT: diagnostic patterns, case examples and pitfalls. Abdom Imaging 2009; 34:391–402. [Crossref]

27. Li X-F, Civelek A. Severe hypoxia of ascites and increased 18F-FDG uptake in ascites carcinomas: A paradox to Warburg effect. J Nucl Med 2012; 53:1137.

28. Li X-F, Du Y, Ma Y, Postel GC, Civelek AC. 18F-Fluorodeoxyglucose uptake and tumor hypoxia: revisit 18F-Fluorodeoxyglucose in oncology application. Transl Oncol 2014; 7:240–247. [Crossref]

29. Takalkar AM, Bruno GL, Reddy M, Lilien DL. Intense FDG activity in peritoneal tuberculosis mimics peritoneal carcinomatosis. Clin Nucl Med 2007; 32:244–246. [Crossref]

30. Chen CJ, Yao WJ, Chou CY, Chiu NT, Lee BF, Wu PS. Peritoneal tuberculosis with elevated serum CA125 mimicking peritoneal carcinomatosis on F-18 FDG-PET/CT. Ann Nucl Med 2008; 22:525–527. [Crossref]

31. Suri S, Gupta S, Suri R. Computed tomography in abdominal tuberculosis. Br J Radiol 1999; 72:92–8. [Crossref]

32. Sahin H, Isik H, Uygun Ilikhan S, Tanriverdi H, Bilici M. Disseminated tuberculosis in a non immun compromised patient with a complicated diagnosis. Respir Med Case Rep 2015; 14:1–3. [Crossref]

33. Deraco M, Santoro N, Carraro O, et al. Peritoneal carcinomatosis: feature of dissemination. A review. Tumori 1999; 85:1–5. [Crossref]

34. Kang SJ, Kim JW, Baek JH, et al. Role of ascites adenosine deaminase in differentiating between tuberculous peritonitis and peritoneal carcinomatosis. World J Gastroenterol 2012; 18:2837–2843. [Crossref]

35. Han CM, Lee CL, Huang KG, et al. Diagnostic laparoscopy in ascites of unknown origin: Chang Gung Memorial Hospital 20-year experience. Chang Gung Med J 2008; 31:378–383.

36. Lucey BC, Stuhlfaut JW, Soto JA. Mesenteric lymph nodes seen at imaging: causes and significance. Radiographics 2005; 25:351–365. [Crossref]